Chapter 1

Use in Garfield

1.1 Practical aspects

Garfield is written in Fortran-77 and hence can't use arbitrary precision arithmetic when evaluating the series and integrals. Furthermore, care needs to be taken that very large and small numbers do not occur at intermediate stages of the computation. In addition, to be useful from a practical point of view, the evaluation has to be reasonably efficient. This leads to a number of numerical considerations which are discussed in this paragraph.

1.1.1 Computing I_n, K_n, I'_n and K'_n

The higher order modified Bessel functions are computed using the recursion relations

$$K_{n+1}(x) = K_{n-1}(x) + 2nK_n(x)/x \tag{1.1}$$

$$I_{n+1}(x) = I_{n-1}(x) - 2nI_n(x)/x. \tag{1.2}$$

Due to the minus sign in the recursion relation for I_n, inaccuracy related errors diverge with n. One therefore applies the recursion from large order downwards, a technique also known as Miller recursion. Assuming I_N is the highest order term one needs, one sets $I_{N+3} = 0$ and $I_{N+2} = \epsilon$ and uses

$$I_{n-1}(x) = I_{n+1}(x) + 2nI_n(x)/x$$

to obtain initial values down to I_0. These initial values are rescaled by multiplying the entire series with a common factor which puts I_0 at the correct value. Starting from essentially arbitrary values for I_{N+3} and I_{N+2} may seem awkward, but it is readily shown that the values for lower orders are barely influenced by this choice.

All terms that appear in the formulae for the potential and field have one of three structures:

$$I(x)\ I(x')\ K(y)/I(y) \qquad x, x' < y \tag{1.3}$$

$$K(x)\ K(x')\ I(y)/K(y) \qquad x, x' > y \tag{1.4}$$

$$I(x)/K(x)\ K(y)/I(y). \tag{1.5}$$

One can't evaluate these terms directly for large x and y since the modified Bessel functions I_n and K_n have an exponential asymptotic behaviour as function of their argument, but the products are well behaved if $x,\ x' \approx y$ so that the exponentials approximately cancel. We therefore factorise these functions as

$$I_n(x) = \mathrm{e}^{x} i_n(x) \tag{1.6}$$
$$K_n(x) = \mathrm{e}^{-x} k_n(x) \tag{1.7}$$

where $i_n(x)$ and $k_n(x)$ are of polynomial order. The functions $i_0(x)$, $i_0(x)$, $k_0(x)$ and $k_1(x)$ are supplied by various numerical libraries and the recursion relations apply to i_n and k_n the same way they do to I_n and K_n.

The derivatives of the modified Bessel functions are computed from the relations

$$I_n'(x) = (I_{n+1}(x) + I_{n-1}(x))/2 \tag{1.8}$$
$$K_n'(x) = -(K_{n+1}(x) + K_{n-1}(x))/2 \tag{1.9}$$

using $I_0'(x) = I_1(x)$ and $K_0'(x) = -K_1(x)$ as calibration points. Also these relations hold for the factorised functions i_n and k_n.

1.1.2 Summing

At constant x, $I_n(x)$ decays and $K_n(x)$ rises asymptotically faster than $\exp(n)$ and slower than $\Gamma(n)$. The same goes for $i_n(x)$ and $k_n(x)$. The precise rate depends on x. Asymptotic formulae have been devised for various domains of x and n, but none of them is sufficiently simple to be used for factorisation in our context. A first limit on n is therefore imposed by the requirement that $i_n(x)$ and $k_n(x)$ can be computed without numeric under- and overflow. This is in practice simple since one can monitor the values while applying the recursion relations, but this is of course no guarantee that the series has converged. Conditions for this follow from a closer examination of the expressions.

If $x = x' = y$, then all terms in Eq. 1.3 and 1.4 have the form $I_n(x)K_n(x)$ which decreases slower than $1/n$ for all x and n relevant in the present context, and the related series do not converge therefore. Translated into geometry, this means that the convergence of the series is problematic if the charge and the measurement point are both located near a wire or a tube.

As soon as $x, x' < y$ in Eq. 1.3 or $x, x' > y$ in Eq. 1.4, the terms decay exponentially and convergence is assured. The number of terms needed to achieve a certain precision depends strongly on the ratios x/y and x'/y as well as on the absolute magnitude of x, x' and y. Given the complex asymptotic behaviour of the modified Bessel functions, we do not attempt to estimate the required number of terms a priori, but rather stop summing as soon as the terms being added contribute less than the numeric accuracy to the sum.

In practical applications, the number of terms ranges from $1 - 2$ for well separated charges, measurement points and electrodes, to $40 - 50$, the highest orders that can be computed without under- and overflow.

Since the required number of terms depends on the value of the integration parameter, we perform the summing inside the integral rather than vice-versa.

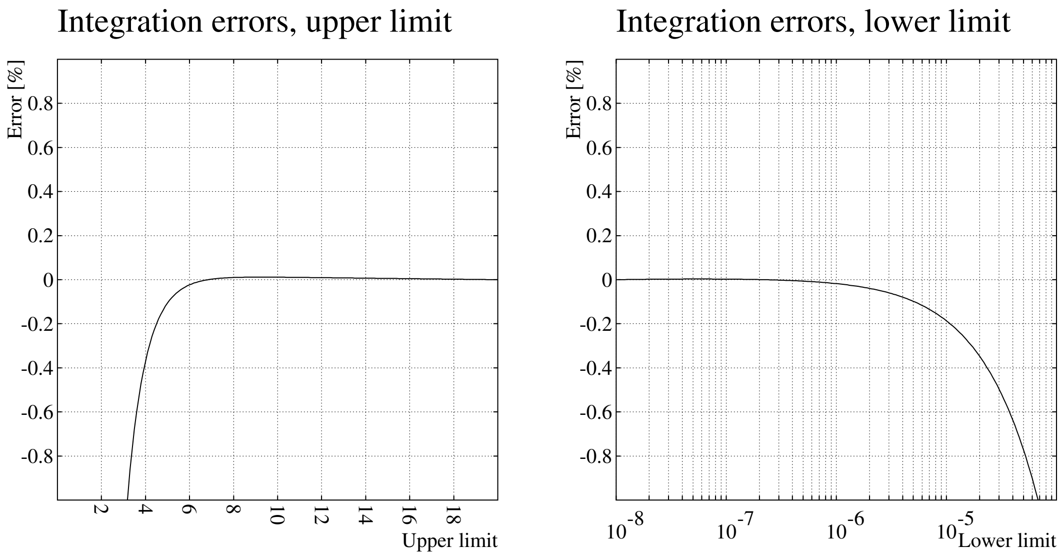

Figure 1.1: The left graph shows the error introduced by the upper limit on λ, expressed as the logarithm of the exponential factor of the largest term in the potential formula. In this case a wire potential has been used, which has only one term, and the exponential factor equals $\exp(-\lambda(\rho/r_{\mathrm{w}} + \rho'/r_{\mathrm{w}} - 2))$ where r_{w} is the wire radius. The graph on the right shows the error due to the lower limit on λ which is expressed as a fraction of the upper limit.

1.1.3 Integrating

Integration is done using 6-point Gauss quadrature over a number of subdivisions of the range $\lambda_{min} \leq \lambda \leq \lambda_{max}$.

At large λ, the integrands tend to zero. We choose the upper integration limit λ_{max} such that the exponential factor of the largest term is equal to $\exp(-20)$ for $\lambda = \lambda_{max}$.

The integrands are divergent when approaching $\lambda = 0$. Since the divergence is of logarithmic order, it doesn't contribute substantially to the integral. In Garfield, the divergence is avoided by using a lower integration limit $\lambda_{min} = 10^{-6}\lambda_{max}$.

As illustrated in Fig. 1.1, the inaccuracy introduced by these limits is typically less than $10^{-3} - 10^{-4}$.

1.1.4 Flux integration around a charge

(Plots to be added)

1.2 Application

1.2.1 High rate gaseous detectors

High energy physics employs a wide variety of particle detectors. Gaseous detectors, one class of particle detectors, rely on the production of ionisation electrons when charged particles traverse a gas mixtures. The ionisation electrons thus produced are attracted by electrodes located in the gas and placed at a high positive potential. Since these electrodes are generally small, of order $10 - 100\ \mu\mathrm{m}$, the fields in their vicinity are large, typically over $100\ \mathrm{kV/cm}$. As a result, the ionisation electrons acquire sufficient energy during their approach to further ionise the gas and hence produce an avalanche of $10^4 - 10^5$ electrons and ions. The ions and electrons produced in the process, move at a sufficient speed to induce measurable currents in the electrodes.

The avalanche electrons are evacuated in a few nsec through the electrodes, but the ions are ≈ 1000 times slower and have to travel a much longer distance before they too can be evacuated. They typically stay around for several $10\ \mu\mathrm{sec}$, if not longer.

Since the detectors in for instance the LHC experiments have to operate in a high rate environment, the ions produced in the avalanches caused by the passage of one charged particle, are not yet evacuated by the time the next charged particle traverses the detector. Hence, a cloud of ions known as space-charge develops in the vicinity of the electrodes. Ultimately, this cloud generates a field which is sufficiently large to reduce the field in which the avalanches develop, thus reducing the avalanche size and hence the measured signal.

At very large rates and low gain in cylindrical counters, the gain reduction can successfully be computed assuming a symmetric space-charge distribution. At lower rates however, the effects can still be sizeable while there are substantial time-dependent fluctuations. It is this domain which is addressed by the calculations presented in this paper.

1.2.2 Atlas MDT

Applied to the Atlas muon chambers (MDT), one finds the potential contours shown in Figs. 1.2, 1.3 and 1.4. One notes that in the vicinity of the wire, the coaxial potentials are a good approximation of the wire potentials.

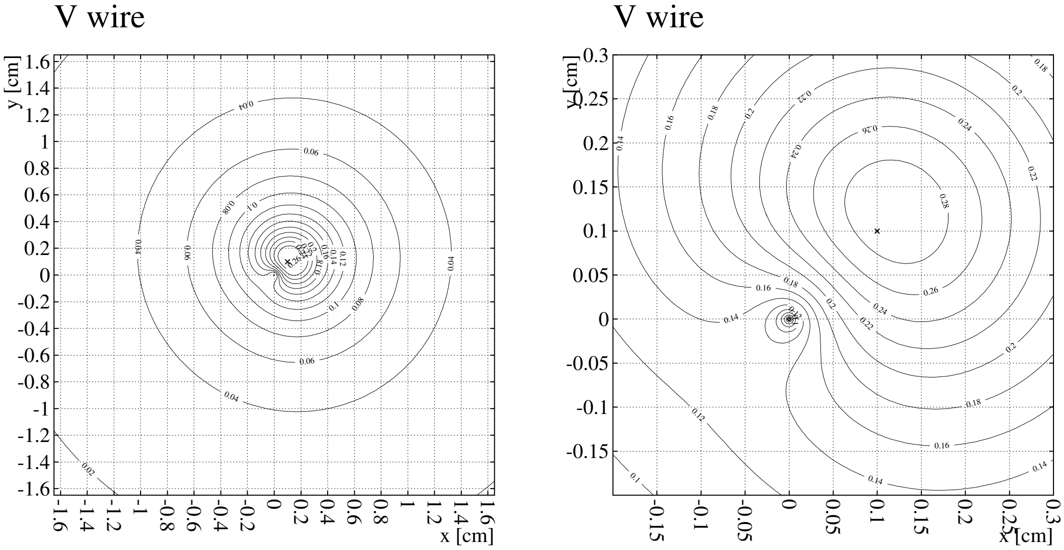

Figure 1.2: Wire potentials computed around a $30\ \mu\mathrm{m}$ diameter wire at $(0, 0)$ mm with a point charge at $(1, 1, 2)$ mm. The wire is earthed.

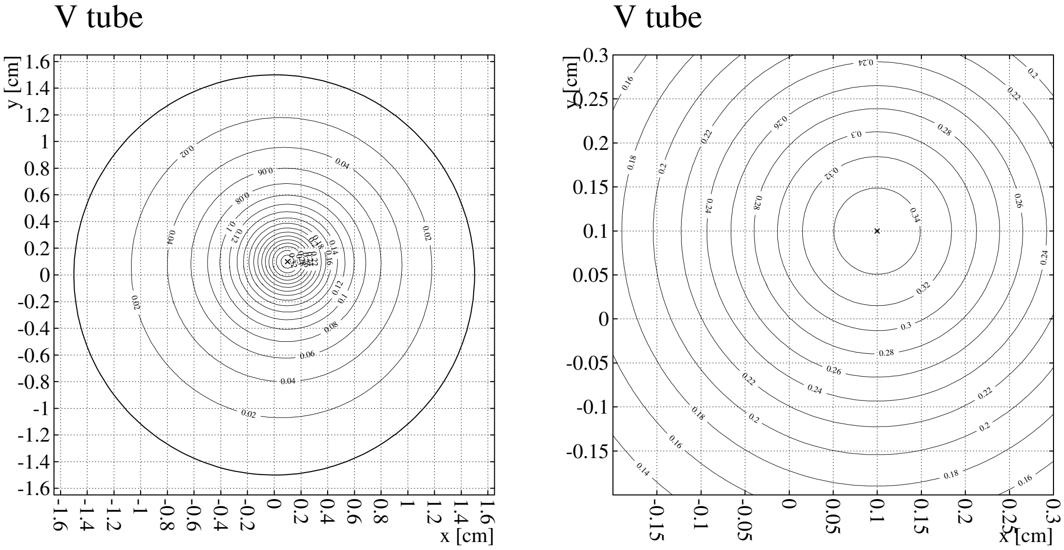

Figure 1.3: Tube potentials computed for the inside of a 30 mm diameter tube with a point charge at $(1, 1, 2)$ mm. The tube is earthed.

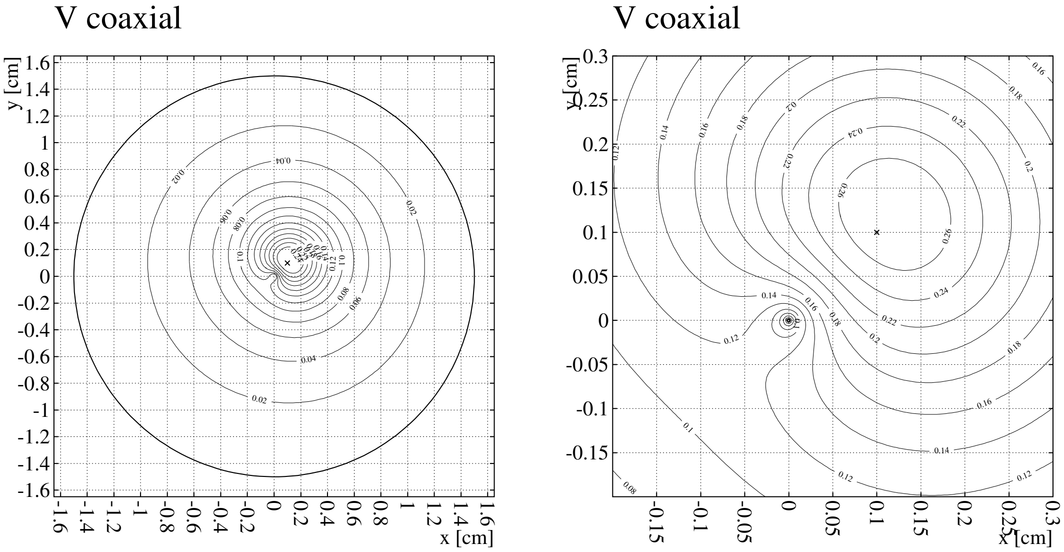

Figure 1.4: Coaxial potentials computed for the Atlas MDT's which have a 30 μm diameter wire at $(0, 0)$ mm, a 30 mm diameter tube and a point charge at $(1, 1, 2)$ mm. The wire and the tube are earthed.